A sensitive and reproducible *in vivo* imaging mouse model for evaluation of drugs against late stage human African trypanosomiasis.

Hollie Burrell-Saward[1], Jean Rodgers[2], Barbara Bradley[3], Simon L. Croft[1], Theresa H. Ward[1#].

[1] *Department of Immunology and Infection, Faculty of Infectious and Tropical Diseases, London School of Hygiene and Tropical Medicine. London WC1E 7HT, UK*

[2] *Institute of Biodiversity, Animal Health and Comparative Medicine, College of Medical, Veterinary and Life Sciences, University of Glasgow, Glasgow G61 1QH*

[3] *Institute of Infection and Inflammation, College of Medical, Veterinary and Life Sciences, University of Glasgow, Glasgow G61 1QH*

[#]Corresponding author. Tel: 020 7927 2649; Email: theresa.ward@lshtm.ac.uk

Short running title: *In vivo* imaging of anti-trypanosomal drug evaluation

Keywords: Human African trypanosomiasis, *Trypanosoma brucei brucei*, mouse model, bioluminescence imaging, luciferase.

Abstract

Objectives: To optimise the *Trypanosoma brucei brucei* GVR35 VSL-2 bioluminescent strain as an innovative drug evaluation model for late stage human African trypanosomiasis.

Methods: An IVIS$^{®}$ Lumina II imaging system was used to detect bioluminescent *T. brucei brucei* GVR35 parasites in mice to evaluate parasite localisation and disease progression. Drug treatment was assessed using qualitative bioluminescence imaging and quantitative PCR.

Results: We have shown that drug dose-response can be evaluated using bioluminescence imaging and confirmed quantification of tissue parasite load using qPCR. The model was also able to detect drug relapse earlier than the traditional blood film detection and even in the absence of any detectable peripheral parasites.

Conclusions: We have developed and optimised a new, efficient method to evaluate novel anti-trypanosomal drugs *in vivo* and reduce the current 180-day drug relapse experiment to a 90-day model. The non-invasive *in vivo* imaging model reduces the time required to assess preclinical efficacy of new anti-trypanosomal drugs.

Introduction

Human African trypanosomiasis (HAT), or sleeping sickness, is caused by the vector-borne protozoan parasites *Trypanosoma brucei gambiense* and *Trypanosoma brucei rhodesiense,* with the subspecies giving rise to different clinical features and progression of this multi-stage disease. Fewer than 8000 cases were reported in 2013,[1] but almost 70 million people are exposed to the risk of the parasite infection within the African continent every year.[2,3]

The disease manifests in two stages: (i) an early stage, which is often referred to as the haemolymphatic stage with parasites present in the blood, lymph and peripheral tissue, and (ii) a later 2nd stage that follows invasion of the central nervous system. Early and late stages are treated by different anti-trypanosomal drugs.[4] Patients typically present with late stage HAT due to the non-specific nature of early stage symptoms. However, chemotherapeutic intervention at the late stage is not straightforward, being limited by the requirement of hospitalisation for parenteral dosing and inherent drug toxicity.[5]

Drug development has been slow, partially due to the length of *in vivo* testing that is involved. Two new compounds are in clinical trials (fexinidazole and SCYX-7158). Currently the mouse models involved in HAT drug development are either for the early stage of the infection, using the monomorphic line *T. b. brucei* Lister 427 (or a derivative), or for the late stage, using the 'gold standard' pleiomorphic strain *T. b. brucei* GVR35.[6] GVR35 is commonly used to study CNS infection and assess drug therapies for the late stage of the disease, as these trypanosomes cross the blood brain barrier and limit outbred mice to a survival time of 30 days post-infection. The standard drug relapse method follows a 180-day infection protocol.[7]

Bioluminescence imaging can provide highly sensitive, non-invasive detection of parasite distribution in a mouse model that can be followed in a single animal for the entirety of the experiment and removes the need for extra animal groups for each time point. Parasites labelled with bioluminescent reporters that emit light in the blue and green part of the spectrum, have encountered problems with high levels of tissue absorption, resulting in poor signal detection in deep tissue.[8] By using red-shifted

proteins, an improved level of signal can be detected as light absorption by tissues is minimised, therefore providing more sensitive parasite detection than traditional blood films.[9,10]

An initial bioluminescent model using green light-emitting luciferase expressed in GVR35 was developed to study HAT in a mouse model.[10] Further to the use of GVR35 LUC-2, a red-shifted bioluminescent *T. b. brucei* strain, GVR35 VSL-2, was developed.[9] This strain was shown to have a bioluminescence 1000-fold higher than the GVR35-LUC2 strain, with a much higher sensitivity that allows detection of 100 trypanosomes or fewer *in vivo*.[9]

We describe here a highly sensitive bioluminescence model, utilising the GVR35 VSL-2 strain to evaluate trypanocidal compounds and to determine drug relapse earlier than the current 180-day 'gold-standard' model. In addition this system reduces the number of animals required in comparison to the wild-type model and is able to evaluate and give a dose response on drugs by 35 days post-infection. Overall, use of this improved system shortens experiments from 180 to 90 days, which could significantly enhance drug development for HAT.

Materials and Methods

<u>Animals and Ethics</u>

Female CD1 mice in range of 20-25 g (Charles River, Margate, UK) were housed in groups no larger than five in specific pathogen-free individually vented cages, and were fed *ad libitum*. All work was carried out under the approval of the UK Home Office Animals (Scientific Procedures) Act 1986 and the London School of Hygiene & Tropical Medicine Ethics Committee. ARRIVE guidelines are followed in this report[11].

<u>Parasites</u>

The strains used were wild-type (WT) *T. b. brucei* GVR35 and the transfected *T. b. brucei* strains GVR35 VSL-2 and GVR35 LUC2.[9,10] The wild-type produces a chronic infection in mice,[12] and was used to validate the bioluminescent transfected strain.

<u>Infection</u>

Mice were infected as per Kennedy *et al* with minor modifications.[6] 5×10^3 trypanosomes/mL from a donor mouse were diluted in phosphate buffered glucose saline pH 8.0 as described,[7] injected into mice by the intravenous route (i.v.) and randomised into cages of 5. For neuropathological evaluation, mice were infected by intraperitoneal injection (i.p.) of 3×10^4 *T. b. brucei* GVR35 WT, LUC2, or VSL-2 strains.

At the end of an experiment, blood was collected via cardiac puncture and mixed with a chaotropic salt (guanidine HCl) in a 50/50 solution and stored at 4°C for DNA extraction and qPCR. For *ex vivo* imaging and qPCR analysis of the brains, mice were perfused with phosphate buffered saline (PBS) to remove blood, and the brains were snap frozen on dry ice and stored at -80°C for later DNA extraction and qPCR.

In vivo bioluminescence imaging

Infected mice were monitored every 7 days via blood microscopy and by whole animal imaging (all VSL-2 mice and a control group of WT mice). Mice were injected intraperitoneally with the luciferase substrate D-luciferin at 150 mg/kg (Perkin Elmer, Beaconsfield, UK diluted in Dulbeccos Phosphate Buffered Saline) and imaged using a standard set of exposure times in an IVIS® Lumina II (Perkin Elmer) under anaesthesia (2% isofluorane/O_2 mix at 2.5 L/min). All images were acquired using the following exposure times; 1, 3, 10, 30, 60 and 180 seconds, with medium binning, 1 f/stop and an open filter, and field of view E (12.5 x 12.5 cm). Bioluminescence was quantitated with Living Image® v.4.2 software (Perkin Elmer) and corrected for background bioluminescence.

To confirm CNS infection, *ex vivo* imaging of perfused brains was performed. Prior to imaging, 50 µL of 15 mg/mL luciferin was pipetted onto the brain and imaged using the settings as above.

Real-time quantitative PCR to determine parasite load.

Real-time quantitative PCR was used to determine parasite load in cardiac blood and perfused brain material, using a primer sequence to target the invariant surface glycoprotein (ISG-75).

DNA was extracted from whole brain homogenate and cardiac blood using Roche High Pure PCR template according to the manufacturer's instructions (Roche, Burgess Hill, UK) and quantified by Nanodrop (ThermoFisher Scientific, Loughborough, UK).

Standards for the gene ISG-75 were generated by conventional PCR from *T. b. brucei* GVR35-derived cDNA, followed by purification using the QIAquick PCR Purification Kit (Qiagen, Crawley, UK). Copy numbers were calculated based on the fragment length, and standards were used in subsequent assays to generate standard curves ranging from 10^8 copies to 10 copies/reaction. The levels of ISG-75 in the indicated samples were measured by real-time quantitative PCR using SYBR® Green (Applied Biosystems by Life Technologies, Paisley, UK) incorporation in an ABI Prism 7000 sequence detection system (Applied Biosystems) relative to the standard curve. Each reaction was

performed in duplicate with 4 µL DNA, 10 µL SYBR® Green master mix, 0.2 µL each primer (final concentration 200 nM), and 5.6 µL water, to produce a reaction volume of 10 µL. PCR conditions were 10 min 95°C denaturation step, followed by 40 cycles of 95°C: 15 s / 60°C: 1 min / 72°C: 1 s.

Primer sequences were: ISG FW: 5'-TTGCTGATAAAGTTGCAGAGGA-3', and

ISG RW: 5'-CAACTCGAACTCTATATAACCAGCA-3'

Neuropathological evaluation

The severity of the pathological reaction within the brain of mice infected with GVR35 WT was evaluated and compared with the VSL-2 strain as well as the recently described LUC2 strain.[10] This was carried out to ensure that there were no overt differences in neuropathogenesis between the genetically modified strains and the WT parasite. The mice were euthanized at 7, 14, 21 and 28 days post-infection and the brains were extracted and fixed in 4% neutral buffered formalin. The tissue was then embedded in paraffin wax, sectioned and stained with haematoxylin and eosin (H&E). The severity of the reaction was assessed by two independent assessors in a blinded fashion using a previously defined grading scale.[6]

In vivo drug efficacy and relapse evaluation

Mice were infected as described above. A CNS control group treated with analytical grade diminazene aceturate, DA (Sigma-Aldrich, Poole, UK) at 40 mg/kg intraperitoneally, which clears peripheral parasitaemia, and a negative control group of untreated infected mice was included for both strains. Mice were randomised into groups of five with a single group per drug/dose.

Melarsoprol is difficult to dissolve for administration, therefore, with advice from Pharmidex (Stevenage, UK), we used an IV formulation consisting of 10% v/v 1, 3-Dimethyl-2-imidazolidinone (Sigma-Aldrich), 10% v/v 1-Methyl-2-pyrrolidinone (Sigma-Aldrich), 35% v/v propylene glycol (Sigma-Aldrich) and 45% v/v 50 mM glycine/HCl (Sigma-Aldrich), which was then diluted to 10%

v/v in 5% dextrose solution. Melarsoprol (Sanofi, Paris, France) was diluted in this IV formulation and administered at four dose-response concentrations (10, 6, 3, 1 mg/kg) over a four day period from D21-24 inclusive. Mice were monitored via imaging and blood films (from the tail vein) every 4-5 days until D35. At D35 mice were culled and qPCR analysis carried out on blood and brain samples to determine ED_{50} and ED_{90} values.

To assess relapse, two doses (10 mg/kg and 6 mg/kg) from the drug efficacy experiment were used and following the same protocol as described above, mice were infected and dosed. Mice were imaged and blood films (from the tail vein) taken every 7 days from D35 to D180. Mice were culled when humane endpoints (weight loss greater than 10% total body weight and hind-leg paralysis) of the experiment were reached.

Results

Validation of bioluminescence model

To ensure that the VSL-2 model exhibits the same kinetics of infection as the wild type GVR35, a direct comparison between the two strains was carried out using the standard 35-day study as described by Kennedy.[13]

At D7 post-infection bioluminescence signal was patchy throughout the mouse, but resided predominantly in the lower back region and lymph nodes (Fig. 1a). The trypomastigotes continued to multiply and spread throughout the blood and lymphatic system and, on D14, signal was observed throughout the animal. By D21 a similar signal distribution was seen, although the bioluminescence was much higher, peaking at 1×10^8 photons/second. From the heat-map scale it can be seen that the liver/spleen area displays the highest bioluminescence (Fig. 1a), providing further evidence that the lymphatic system is heavily infected.

Following treatment with DA at D21, overall bioluminescence in infected animals imaged at D28 was greatly reduced, with a focal signal found only in the head region, as the clearance of peripheral parasitaemia revealed possible CNS infection. By D35, the bioluminescence signal in the head region became more intense, as the cranial concentration of parasites appeared to increase, with a 10-fold increase in flux between D28 and D35. The control wild type mouse showed no bioluminescence.

Quantitation of total flux revealed that as the infection progressed the bioluminescence increased from 10^8 to just under 10^{10} total flux until DA treatment was administered (Fig. 1b). In comparison parasitaemia was not detectable via microscopy until D14 and then was undetectable following treatment with DA (Fig. 1b). It remained undetectable until the end of the experiment at D35 despite bioluminescence signal clearly apparent in the head.

To confirm the presence of trypanosomes in brain tissue following whole animal imaging at D35, the mice were perfused to clear the tissue of blood, and brains were excised and imaged *ex vivo* (Fig. 1c). Bioluminescence was detectable in all VSL-2-infected mouse brains and was comparable to the signal

seen in the head region of the respective intact mice at D35 (Fig. 1a). In the brain of mouse 2, the signal was most prominent in the olfactory bulb of the brain whereas in mouse 1 and 3 the signal non-specifically disseminated through the entire brain, with mouse 3 showing a high signal (red 'hot spot') in the cerebellum. The remainder of the infected group showed similarly non-specific distribution of bioluminescence in the brain (not shown).

Following *ex vivo* imaging, DNA was prepared from the perfused brains and quantitative PCR was used to determine the parasite load in each brain (Fig. 1c). Comparing qPCR to bioluminescence signal, the total flux was representative of the number of trypanosomes present. The brain of mouse 3 had areas of higher flux and therefore had an overall higher quantity of trypanosomes present. However, in the brains of mouse 1 and 2, despite showing differences in the distribution of parasites, a trend can be identified between parasite burden as determined by qPCR and bioluminescence. The control wild type-infected brain had no bioluminescence but high parasitaemia.

To determine whether parasite transfection had interfered with invasion and neuropathological effects in the brain,[6] a well-established neuropathology grading scale was used to assess the severity of the neuropathological response over the course of infection of 28 days (Fig. 2). VSL-2 was compared to the current bioluminescence model LUC2 and to WT. The results show that there was no significant difference between the neuropathological response to infection for the VSL-2 and wild type strains.

Drug efficacy of melarsoprol in the treatment of *T. b. brucei* GVR35 VSL-2

To extend the potential of a drug evaluation model, the ability to determine dose response, as well as relapse could provide an improved knowledge of drug efficacy. Infected mice were treated with melarsoprol at varying doses as indicated to provide a dose response and at D21, 24, 28, 30 and 35, bioluminescence and parasitaemia were measured (Fig. 3). The bioluminescence and parasitaemia fell (Fig. 3b) immediately after treatment (D24 post-infection). Mice treated with 1 mg/kg melarsoprol, demonstrated an immediate clearance after treatment but, by D30, bioluminescence signal was detectable and was focused to the head and spinal region of the mouse (Fig. 3a). The bioluminescence continued to increase and at D35 reached 100-fold greater than background (as determined by the

average bioluminescence obtained from WT mice) at 10^8 photons/second and was disseminated throughout the entire animal. Although bioluminescence was detectable from D30 in the low dose melarsoprol treatment, peripheral parasitaemia could only be detected in these mice when the infection re-disseminated throughout the animals at D35 (Fig. 3a, b).

A single 40 mg/kg dose of DA showed an initial drop in bioluminescence, with signal limited to the head region (as shown in Fig. 1a) before increasing over the remaining 11 days (Fig. 3b). Unlike the low dose melarsoprol-treated mice, peripheral parasitaemia was undetectable in blood films, suggesting the signal originated from organs or the lymphatic system. No recovery of bioluminescence was seen in mice treated at higher doses of melarsoprol within this time course.

At D35 mouse brains were removed and qPCR analysis carried out to determine the quantity of trypanosomes present after drug treatment. The detection limit of the qPCR was 50 trypanosomes/50 ng of DNA. A clear dose-response effect was observed (Fig. 3c), with the increasing dose of melarsoprol reducing the number of trypanosomes present to below the detection limit. DA showed a high number of trypanosomes in the brain although with a reduction in parasite load compared to the untreated control, further confirming that DA was unable to clear parasites in the CNS to a curative level. The qPCR data of melarsoprol-treated brains correlates with the whole animal and *ex vivo* imaging data, and provides evidence that bioluminescence can be used to determine dose response effect.

Non-invasive monitoring of drug relapse

To investigate the potential of the VSL-2 model to study drug relapse, mice infected with GVR35 VSL-2 were treated with melarsoprol at curative (10 mg/kg) and non-curative (6 mg/kg) doses administered i.v. The bioluminescence and parasitaemia for each individual mouse was then followed through a 180-day study (Fig. 4).

Parasitaemia for the mice dosed with 6 mg/kg (Fig. 4a) was undetectable prior to D63 in any animal, at which point low numbers of parasites were detectable in the blood of 4 of the 5 animals, after which parasitaemia increased. Mouse 5 remained aparasitaemic (according to blood films) during the

119 days showing few symptoms other than splenomegaly before being culled. In comparison, the bioluminescence data for this group of mice appears very different. Signal was detected as early as D49 for 3 of the 5 mice, and by D63 signal was observed in the remaining mice. Unlike the parasitaemia data for the same mice, the bioluminescence fluctuated during the 56-day period prior to the termination of the group at D119. Therefore, despite there being no detectable peripheral parasitaemia for mouse 5, bioluminescence was still detected in all mice in the 6 mg/kg group.

Immediately after treatment of 10 mg/kg melarsoprol, blood films indicated that the parasitaemia had cleared in all mice. Four of the five mice remained negative throughout the 180 days, but mouse 2 had parasitaemia at D91 of 14 trypanosomes/10 fields of view before decreasing and then reappearing again at D112 before being culled at D119 as the mouse became lethargic (Fig 4b). In contrast, the bioluminescence data for 10 mg/kg shows that relapse occurred in mouse 2 much earlier, at D70 (Fig. 4b), with a total flux of 4.64×10^6 photons/seconds (10-fold increase on the background) before falling below background detection, and then following a pattern of decreasing and increasing bioluminescence before a spike at D119 of 1.27×10^{10} photons/second, when the mouse reached its humane endpoint. The bioluminescence approach was therefore able to detect drug relapse much earlier than traditional blood film.

Discussion

The current pre-clinical drug evaluation model requires mice to be monitored for up to 180 days post-infection, with relapse being detected when parasites re-establish an infection in the periphery, detectable in blood films.[6] This model is unable to detect viable parasites in other organs such as the brain, without mice being sacrificed and the tissues removed for further analysis. The experimental time period of six months is not appropriate for drug development and a new innovative approach is required to speed up the process and provide data on time-to-kill and differential effects on parasite distribution. At present there is no current model for assessing dose response drug efficacy, as it is not possible to determine the level of parasite persistence within tissues using contemporary techniques.

Bioluminescent model systems utilising luciferase have been described for the assessment of drugs for other diseases and infections.[14-16] The progress made with both the LUC2 model and development of the red-shifted VSL-2 strain, has paved the way for a new mouse model of HAT that is both highly sensitive and non-invasive. Preliminary studies on GVR35 VSL-2 showed that the model produces similar infection to the wild type strain and that bioluminescence can be detected in the brain by both whole animal and *ex vivo* imaging.[9]

VSL-2 provides higher imaging sensitivity than previous transfected trypanosome strains,[9,10] and it is this that enables a dose-response effect to be detected in whole mouse imaging after treatment with melarsoprol. While the LUC2 model provided a substantial improvement on the currently used GVR35 wild type model,[10] the greater sensitivity and detection limit of the VSL-2 model as determined in this study allows bioluminescence to be used to determine a dose response effect, and analysis of excised brains using PCR corroborates this. Furthermore, the i.v. infection route provides a tightly reproducible infection determined by bioluminescence detection, even in the outbred mouse line used. A shortened experimental time of 35 days is sufficient to confirm anti-trypanosomal activity on stage 2 HAT by loss of bioluminescence in the brain, something that has been difficult to determine *in vivo* before now.

The greater sensitivity of the bioluminescence approach is demonstrated further in the analysis of drug relapse. By D60 there is a clear indication of subcurative clearance (in this case 6 mg/kg) and by 90 days relapse is evident, resulting in the reduction of experimental time by 50%. The model also provides an option to extend the time required to follow the animals with minimal invasion due to the non-invasive nature of bioluminescence imaging. Although 10 mg/kg appeared as a curative dose in 4 of the 5 mice through measurement of peripheral parasitaemia and bioluminescence, in one mouse (mouse 2) it was clear from the bioluminescence that parasites could persist long after treatment with increasing flux around D60 and then again at D81 to D112 suggesting relapse. Early studies on melarsoprol also showed that the regimen of 10 mg/kg x 3 days i.v., gave no relapse in peripheral parasitaemia detected by blood films, but two-thirds of the mice in the study died.[17] Poltera concluded that melarsoprol was curative as no parasites were found in the circulating blood or brain tissue in all of the mice as determined by histopathological study and immunofluorescence.[17] The data we have shown here supports that peripheral parasitaemia was not detected, but bioluminescence re-emerged after treatment in one of the five mice through the 180 day experiment, lending further evidence that the lymphatic system is involved in parasite invasion and also raises question on how 'cure' can be defined in the mouse model.

In summary, we have presented evidence here that the red-shifted bioluminescent GVR35 VSL-2 model has the capability of providing a far more sensitive drug assessment system by non-invasive imaging, with the ability to reduce initial screening time by 120 days. In addition to this, the high sensitivity of the imaging combined with quantitative methods of qPCR, have allowed a new methodology to be developed that can assess drug efficacy in terms of ED_{50} and ED_{90} values of novel drugs for treatment of late stage of human African trypanosomiasis. The overall reduction in drug evaluation time and more comprehensive data that can now be determined for pre-clinical drugs will speed up drug development and aid the ongoing progress to HAT elimination.

Transparency declarations

None to declare

References

1.   WHO. Control and surveillance of human African trypanosomiasis. Italy: World Health Organisation, 2013.

2.   Brun R, Blum J, Chappuis F *et al*. Human African trypanosomiasis. *Lancet* 2010; **375**: 148-59.

3.   WHO. Human African Trypanosomiasis. http://www.who.int/trypanosomiasis_african/en/ (3 March 2014, date last accessed).

4.   Pentreath VW, Kennedy PGE. Pathogenesis of Human African Trypanosomiasis. In: Maudlin I, Holmes PH, Miles MA, eds. *The Trypanosomiases*. Oxfordshire: CABI Publishing, 2004; 283-303.

5.   Barrett MP, Croft SL. Management of trypanosomiasis and leishmaniasis. *Br Med Bull* 2012; **104**: 175-96.

6.   Kennedy PGE, Rodgers J, Jennings FW *et al*. A substance P antagonist, RP-67,580, ameliorates a mouse meningoencephalitic response to *Trypanosoma brucei brucei*. *Proc Natl Acad Sci U S A* 1997; **94**: 4167-70.

7.   Jennings FW, Rodgers J, Bradley B *et al*. Human African trypanosomiasis: Potential therapeutic benefits of an alternative suramin and melarsoprol regimen. *Parasitol Int* 2002; **51**: 381-8.

8.   Deliolanis NC, Kasmieh R, Wurdinger T *et al*. Performance of the red-shifted fluorescent proteins in deep-tissue molecular imaging applications. *J Biomed Opt* 2008; **13**: 0440084.

9.   McLatchie AP, Burrell-Saward H, Myburgh E *et al*. Highly sensitive *in vivo* imaging of *Trypanosoma brucei* expressing "red-shifted" luciferase. *PLoS Negl Trop Dis* 2013; **7**: e2571.

10.   Myburgh E, Coles JA, Ritchie R *et al*. In vivo imaging of trypanosome-brain interactions and development of a rapid screening test for drugs against CNS stage trypanosomiasis. *PLoS Negl Trop Dis* 2013; **7**: e2384.

11.   Kilkenny C, Browne WJ, Cuthill IC *et al*. Improving bioscience research reporting: the ARRIVE guidelines for reporting animal research. *PLoS Biol* 2010; **8**: e1000412.

12.   Jennings FW, Whitelaw DD, Urquhart GM. The relationship between duration of infection with *Trypanosoma brucei* in mice and the efficacy of chemotherapy. *Parasitology* 1977; **75**: 143-53.

13.   Kennedy PGE. The pathogenesis and modulation of the post-treatment reactive encephalopathy in a mouse model of Human African Trypanosomiasis. *J Neuroimmunol* 1999; **100**: 36-41.

14.   Barman TK, Rao M, Bhati A *et al*. Non invasive real-time monitoring of bacterial infection & therapeutic effect of anti-microbials in five mouse models. *Indian J Med Res* 2011; **134**: 688-95.

15.   Andreu N, Zelmer A, Fletcher T *et al*. Optimisation of bioluminescent reporters for use with mycobacteria. *PloS ONE* 2010; **5**: e10777.

16.   Claes F, Vodnala SK, van Reet N *et al*. Bioluminescent imaging of *Trypanosoma brucei* shows preferential testis dissemination which may hamper drug efficacy in sleeping sickness. *PLoS Negl Trop Dis* 2009; **3**: e486.

17.   Poltera AA, Hochmann A, Lambert PH. *Trypanosoma brucei brucei*: the response to Melarsoprol in mice with cerebral trypanosomiasis. An immunopathological study. *Clin Exp Immunol* 1981; **46**: 363-74.

Figure Legends

Figure 1. *In vivo* validation of *T. b. brucei* GVR35 VSL-2. Six CD1 mice were infected with VSL-2 via the intravenous route and treated with DA at D21. They were monitored by imaging and blood film acquisition every 7 days until D35 post-infection. (a) Three representative animals of six (M1, M2 and M3) imaged at the indicated time points compared to a mouse infected with wild-type GVR35, showing bioluminescence on a heat-map scale (total flux) where red is an area of high flux i.e., high bioluminescence activity. (b) Quantification of average total flux and parasite number from the six mice in (a). Each data point is a mean ± SD of the bioluminescence analysis and microscopic counts. (c) Mice from (a) were perfused and brains excised and imaged. Excised brains were homogenised and extracted DNA subjected to qPCR, and compared to the bioluminescence.

Figure 2. Comparison of neuropathological effect of bioluminescent strains LUC2 and VSL-2 and wild type. Using the standard neuropathological scoring method,[6] groups of 11-12 brains were haemolysin and eosin stained and sections were evaluated and scored. Graph shows the mean and 95% confidence interval for each group. A Student's *t* test showed that there is no significance between the strains at all time-points, *P* value >0.05.

Figure 3. Determining melarsoprol drug efficacy using bioluminescence and qPCR. Infected CD1 mice were split into groups of six and treated with varying doses of melarsoprol from D21 and monitored until D35. (a) A single representative mouse (1 mouse from group of six) from the top dose 10 mg/kg and low dose 1 mg/kg, showing bioluminescence on a heat map scale (red representing maximum flux) before and after treatment. (b) The average (of six mice) quantification of total flux and parasite number. Each data point is a mean ± SD of the bioluminescence analysis and microscopic counts. Background bioluminescence indicated by stippled line. (c) Brain homogenates from each of the mice from (b) were extracted for DNA and analysed using qPCR. Graph shows mean of six mice ± SD of the number of parasites in 50 ng of DNA.

Figure 4. Early detection of drug relapse of melarsoprol using VSL-2. Mice infected with VSL-2 via the intravenous route were imaged and blood filmed at weekly intervals post-dose of melarsoprol. Graphs show the bioluminescence and peripheral parasitaemia from a group of five mice (M1, M2, M3, M4, and M5) dosed with (a) 6 mg/kg melarsoprol and (b) 10 mg/kg melarsoprol. Values of zero were manually altered to 1 in the parasitaemia counts to enable plotting on a logarithmic scale.
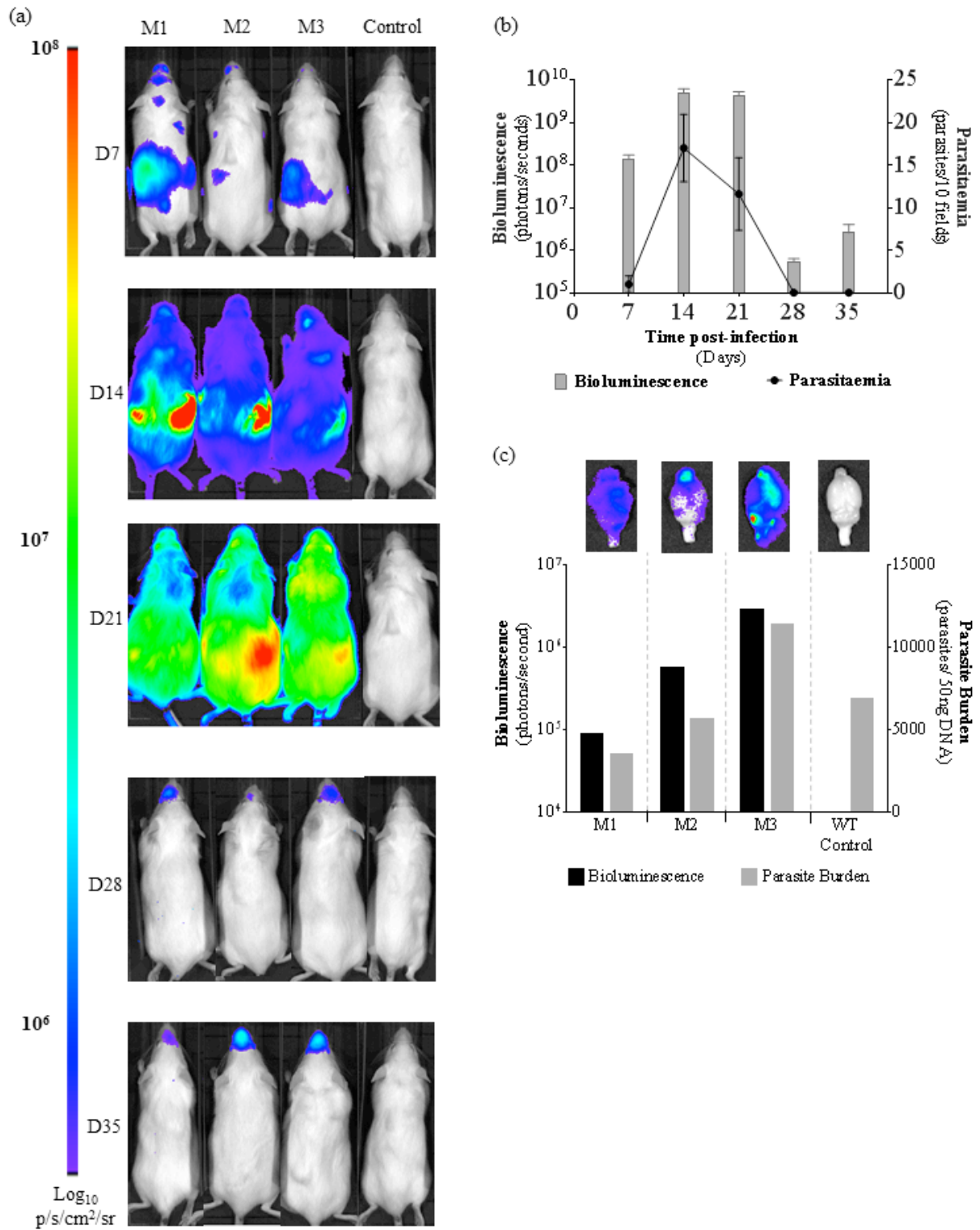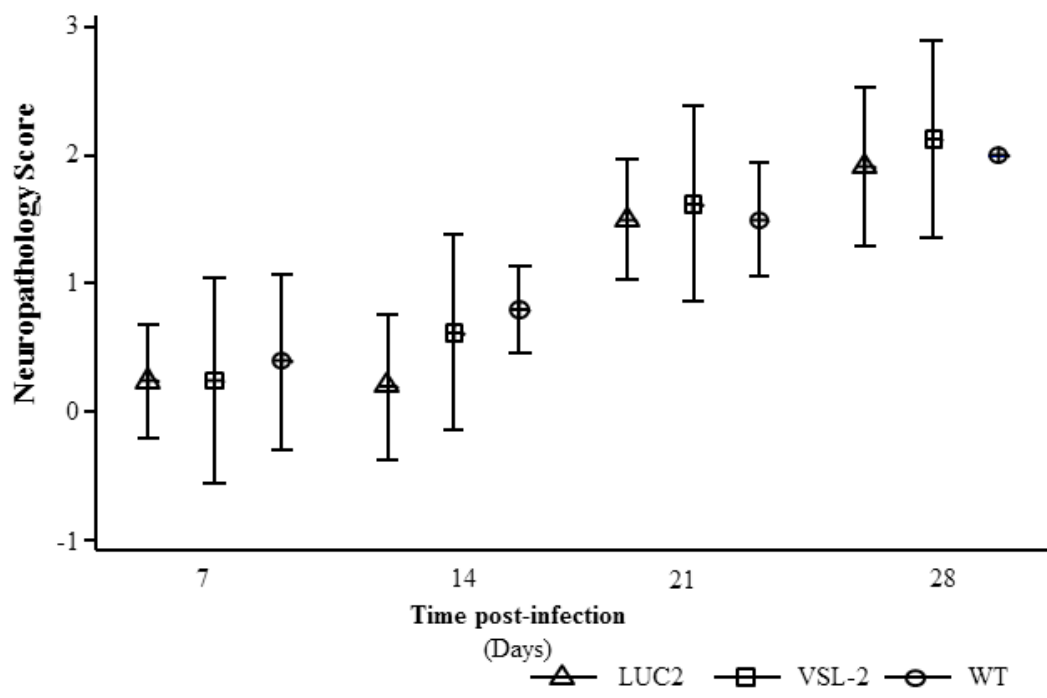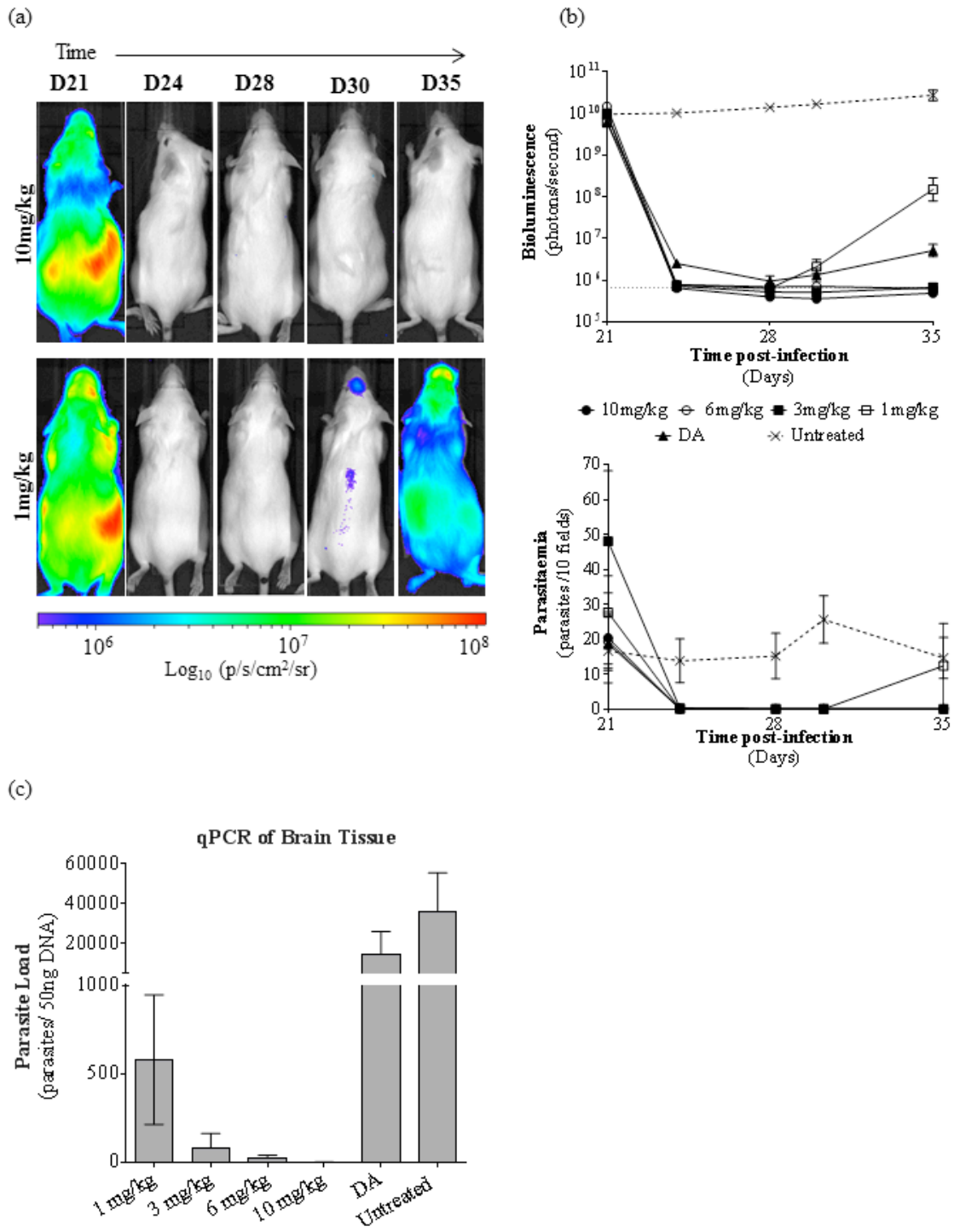
(a)

M1 M2 M3 Control

10^8

D7

D14

10^7

D21

D28

10^6

D35

Log_{10}
$p/s/cm^2/sr$

(b)

(c)

Figure 1

Figure 2

(a)

(b)

(c)

qPCR of Brain Tissue

Figure 3

Figure 4